Mercury concentrations in tuna blood and muscle mirror seawater methylmercury in the Western and Central Pacific Ocean

Romina Vanessa Barbosa, David Point, Anaïs Médieu, Valérie Allain, David P Gillikin, Lydie I E Couturier, Jean-Marie Munaron, François Roupsard, Anne Lorrain

Mercury concentrations in tuna blood and muscle mirror seawater methylmercury in the Western and Central Pacific Ocean

Romina V. Barbosa[1*], David Point[2], Anaïs Médieu[1], Valérie Allain[3], David P. Gillikin[4], Lydie I. E. Couturier[1], Jean-Marie Munaron[1], François Roupsard[3], Anne Lorrain[1]

[1]Univ Brest, IRD, CNRS, Ifremer, LEMAR, F-29280 Plouzané, France

[2]Geosciences Environnement Toulouse (GET) - Institut de Recherche pour le Développement (IRD), CNRS, Université de Toulouse

[3]Pacific Community, Oceanic Fisheries Programme, Nouméa, New-Caledonia

[4]Department of Geosciences, Union College, 807 Union St., Schenectady, NY, 12308, USA

Orcid

Romina Vanessa Barbosa: 0000-0003-1793-8444

David Point: 0000-0002-5218-7781

Anaïs Médieu: 0000-0003-2928-1419

Valérie Allain: 0000-0002-9874-3077

David P. Gillikin: 0000-0003-9874-3077

Lydie Couturier: 0000-0002-3885-3397

Anne Lorrain: 0000-0002-1289-2072

[*]Corresponding authors: Romina Vanessa Barbosa, rominavanessa.barbosa@gmail.com and David Point, david.point@ird.fr

Abstract

Understanding the relationship between mercury in seafood and the distribution of oceanic methylmercury is key to understand human mercury exposure. Here, we determined mercury concentrations in muscle and blood of bigeye and yellowfin tunas from the Western and Central Pacific. Results showed similar latitudinal patterns in tuna blood and muscle, indicating that both tissues are good candidates for mercury monitoring. Complementary tuna species analyses indicated species- and tissue-specific mercury patterns, highlighting differences in physiologic processes of mercury uptake and accumulation associated with tuna vertical habitat. Tuna mercury content was correlated to ambient seawater methylmercury concentrations, with blood being enriched at a higher rate than muscle with increasing habitat depth. The consideration of a significant uptake of dissolved methylmercury from seawater in tuna, in addition to assimilation from food, might be interesting to test in models to represent the spatiotemporal evolutions of mercury in tuna under different mercury emission scenarios.

Keywords

Methylmercury, tunas, blood, white muscle, vertical habitat, Pacific Ocean.

Highlights

Spatial trends of Total [Hg] (THg) concentrations in tuna muscle and blood are identical

Blood to muscle Hg ratio increases with depth habitat of tuna species

Opposed to other tuna, THg was higher in blood compared to muscle in bigeye

THg in blood and muscle mirror seawater methylmercury concentration profiles

Direct uptake of methylmercury by tuna might be more important than currently thought

Introduction

Mercury (Hg) is a global pollutant, mainly present as a gaseous species (Hg^0) in the atmosphere with both natural geogenic (e.g., volcanism), and anthropogenic sources (e.g., coal combustion and artisanal gold mining) (Outridge et al., 2018). A fraction of Hg^0 deposited at the ocean surface as inorganic Hg can be naturally converted into toxic methylmercury (MeHg), mainly produced at depth in oceanic oxygen minimum zones during organic matter remineralization processes (Mason and Fitzgerald, 1990). Methylmercury is a neurotoxic compound for humans and biomagnifies naturally through marine food webs (Bloom, 1992), leading to high concentrations in marine pelagic top predators like tunas and billfishes (Storelli et al., 2002). Fish consumption represents the main human exposure to MeHg (Sunderland, 2007; Sunderland et al., 2018).

The Minamata Convention administrated by the United Nations Environmental Programme (www.mercuryconvention.org) aims to reduce anthropogenic Hg emissions into the environment and to protect human health. The implementation of the Minamata Convention requires the development and coordination of monitoring strategies in various ecosystems and organisms both at the regional and global scales. Yet several key fundamental questions about the Hg cycle remain, in particular the link between atmospheric Hg emissions, seawater MeHg levels and Hg concentrations in marine pelagic predators (e.g., Lee et al., 2016; Medieu et al. 2022). This information is fundamental to better constrain models and predict responses of different Hg emissions scenarios (Wang et al., 2019).

Among top predators, tunas have been particularly studied for their Hg content (e.g., Chouvelon et al., 2017; Houssard et al., 2019; Médieu et al., 2021). Mercury is mainly present as MeHg in tuna muscle tissue (> 91%, Bloom, 1992; Houssard et al., 2019), making the measurement of total Hg (THg) concentrations a suitable proxy of MeHg content. Tunas display relatively high Hg concentrations, sometimes exceeding food safety guidelines (1 $\mu g.g^{-1}$ fresh tissue) (World Health Organization and UNEP Chemicals, 2008), and thus represent the dominant Hg intake in several countries where tuna consumption is high (Sunderland, 2007). Tunas are indeed among the most popular marine species consumed worldwide, and in terms of food and nutrition security, they provide a major source of proteins, essential fatty acids, vitamins, and minerals (Bell et al., 2015; Sirot et al., 2012), in particular in the Western and Central Pacific.

Mercury concentrations in tunas depend of a complex interplay of processes, including physiology (organism's age and size), trophic ecology, habitat, marine biogeochemistry (e.g., in situ MeHg bioavailability), and physics (e.g., ocean currents, light intensity) (Choy et al., 2009; Houssard et al., 2019; Kojadinovic et al., 2007; Wang et al., 2019). A combination of these factors is suspected to drive the spatial variability of Hg concentrations that has been observed in tunas both at the regional (Houssard et al., 2019; Médieu et al., 2022) and global scales (Nicklisch et al., 2017; Tseng et al., 2021). In particular, variable Hg concentrations have been attributed to differences of foraging habitat, with epipelagic species like skipjack (*Katsuwonus pelamis*) and yellowfin tunas (*Thunnus albacares*) exhibiting lower concentrations than bigeye (*T. obesus*) and albacore tunas (*T. alalunga*), which forage deeper in the water column (Choy et al., 2009; Houssard et al., 2019; Olson et al., 2016). This has been associated with the fact that tuna species with enhanced Hg concentrations forage deeper on mesopelagic preys enriched in Hg as they are located closer to deep MeHg production zones (Blum et al., 2013; Madigan et al., 2018). At a regional scale, variations in Hg content in bigeye tuna (by a factor 3) in the south western Pacific has also been attributed to variations of its foraging habitat between locations, with higher Hg content where this species can forage deeper (Houssard et al., 2019).

Studies investigating tuna Hg content have almost exclusively relied on muscle tissue, as it is considered as a storage compartment for MeHg, and because it is also the most edible part of tunas (Houssard et al., 2019; Médieu et al., 2021; Nicklisch et al., 2017). This tissue is suspected to reflect a long but poorly defined period of exposure which may vary among species (Keva et al., 2017). Muscle Hg turnover in captive bluefin tuna (*T. orientalis*) has been estimated to be 2.8 years (Kwon et al., 2016), but it is yet unknown into the wild and has been largely undocumented in tropical tuna species having different lifespan, growth, and metabolic rates (Olson et al., 2016).

Tuna species, in particular bluefin tunas, are considered highly migratory species (Block et al., 2011), and therefore reflect MeHg levels integrated over large transoceanic scales (Tseng et al., 2021). Recent evidence using stable isotopes in tuna muscle tissues indicates that other tuna species such as yellowfin, bigeye, skipjack and albacore, presenting limited spatial migration at the subregional scale, might be more appropriate to capture Hg trends at the local and subregional scales (Houssard et al., 2017; Logan et al., 2020). Carbon and nitrogen stable isotope values ($\delta^{13}C$ and $\delta^{15}N$) are

indeed a suitable tool to infer both local and broad-scale movements and residency patterns of pelagic species (Graham et al., 2010; Logan et al., 2020). Houssard et al. (2017) for example showed that the spatial variability of tuna muscle $\delta^{15}N$ values was similar to the isotopic spatial gradients at the base of the food web (particulate organic matter, and source amino-acid $\delta^{15}N$ values). This illustrates that these tropical tunas were relatively resident at a 6-month to 1-year scale in the Western and Central Pacific Ocean as they are acquiring the isotopic signature of the environment where they forage. However, given the slow Hg turnover expected in muscle, other tissues might be more relevant to picture spatial variations in tunas, in particular blood. Blood circulation plays an important role in the distribution of MeHg across tissues and is expected to be representative of a short exposure time (weeks, e.g., Bearhop et al., 2000). Yet, current knowledge on Hg kinetics and equilibration between blood and muscle tissues in fishes is scant, while necessary to better understand Hg spatial trends especially in tunas exhibiting both horizontal and vertical movements. Comparing Hg concentrations in tissues with different turnover rates could help elucidate the relationship between the history of Hg exposure in tunas with respect to MeHg levels in the water column.

The main objectives of our study were to (i) evaluate the relevance of tuna muscle and blood samples to capture representative geographical trends of Hg concentrations in pelagic ecosystems, (ii) identify the main factors explaining the differences of THg concentrations between four tuna species by evaluating the effect of species, tissue type, biogeochemical province and fish length, and (iii) determine the relationship between local water MeHg profiles and THg concentrations in blood and muscle of tuna species occupying different depth layers of the same region. For objectives (i) and (ii), we determined THg concentrations in muscle and blood tissues from two tuna species, bigeye and yellowfin, in different provinces from the Western and Central Pacific Ocean. Nitrogen isotope values were also measured as another tool to discuss the relevance of blood and muscle tissues to infer spatial patterns of THg concentrations in tunas. For objectives (ii) and (iii), we focused on a smaller region and added samples of albacore and skipjack tunas to discuss the species-specific differences based on their particular physiology and vertical habitat use.

Materials and methods

Study area

Tuna samples were collected from individuals captured within the Western and Central Pacific Ocean, from 145°E to 128°W and 10°N to 26°S (Fig. 1). This region is characterized by four biogeochemical provinces defined by different nitrogen biochemistry at the base of marine food webs, modified from Longhurst (2007) by Houssard et al. (2017): the Archipelagic deep basins modified province (ARCHm), the Warm pool modified province (WARMm), the Pacific equatorial divergence province (PEQD), and the South Pacific Subtropical Gyre modified province (SPSGm). ARCHm is characterized by limited vertical stratification, deep thermocline/oxycline, and enhanced dinitrogen fixation and primary production (Campbell et al., 2005; Moisander et al., 2010; Shiozaki et al., 2014). WARMm presents high sea surface temperatures and a more stratified water column. Primary production in this region is mainly based on regenerated nitrogen (Le Borgne et al., 2011). PEQD presents a strong upwelling from the equatorial undercurrent and the highest primary production of the western and central Pacific Ocean (Chavez et al., 1990). Finally, SPSGm is characterized by ultra-oligotrophic waters, deep thermocline and primary production based mainly on nitrate fixation (Shiozaki et al., 2014).

Tuna sampling and tissue analyses

White muscle and blood tissue samples were collected by trained observers onboard commercial fishing boats (purse seine and longline) between 2001 and 2016 (available dataset: Barbosa et al. 2022, SEANOE). Most of the sampling effort was conducted for bigeye (n= 88, 32 ARCHm + 31 PEQD + 4 SPSGm + 21 WARMm), and yellowfin (n= 60, 45 ARCHm + 1 PEQD + 14 WARMm). A few individuals of albacore (n = 17) and skipjack (n= 5) were also sampled from the ARCHm province. Sampling location (i.e., longitude and latitude) was recorded, as well as sampling date. Fork length was measured to the lowest cm and ranged respectively for bigeye, yellowfin, albacore and skipjack from 42 to 160 cm (85 ± 31, mean ± sd), 49 to 157 cm (114 ± 26), 84 to 101 cm (95 ± 5), and 64 to 81 cm (74 ± 6) (Table S1). Blood was sampled from freshly caught tuna from the incision made by fishermen near the lateral

line (close to the pectoral fin). Samples were frozen onboard, stored at -20°C, freeze-dried and finally ground to a fine and homogeneous powder prior to analyses.

Total Hg concentrations were measured on ~10 mg of powdered, freeze-dried and homogenized samples by thermal decomposition, gold amalgamation and atomic absorption detection (DMA-80, Milestone) at GET (Toulouse, France). Measurements accuracy was checked against different biological standard reference materials (i.e., TORT-2: 0.270 ± 0.060 $\mu g.g^{-1}$, TORT-3: 0.292 ± 0.022 $\mu g.g^{-1}$, DOLT-4: 2.580 ± 0.220 $\mu g.g^{-1}$, and IAEA-436: 4.190 ± 0.360 $\mu g.g^{-1}$) covering a wide range of Hg concentrations. All concentrations are expressed in $\mu g.g^{-1}$ on a dry weight (dw) basis.

Nitrogen stable isotope values were obtained from ~1 mg homogenized freeze-dried samples packed in tin cups and were analyzed using a Costech elemental analyser coupled to an isotope ratio mass spectrometer (Thermo Scientific Delta Advantage with a Conflo IV interface) at Union College (New York, USA). Reference standards (EA Consumables sorghum flour ($\delta^{15}N$ = 1.58 ± 0.15 ‰), in house acetanilide ($\delta^{15}N$ = -0.96 ‰), IAEA-N-2 ammonium sulfate ($\delta^{15}N$ = 20.3 ± 0.2 ‰), and IAEA-600 caffeine ($\delta^{15}N$ = 1.0 ± 0.2 ‰) were used for isotopic corrections, and to assign the data to the appropriate isotopic scale with reproducibility better than 0.1 ‰. Results were reported in the δ unit notation and expressed as parts per thousand (‰) relative to international standards, i.e., atmospheric N_2.

Methylmercury water depth profiles

Water samples were collected using a trace metal clean rosette during the 2015 OUTPACE Cruise (Leblanc and Cornet, 2018) and measured specifically for MeHg at GET (Toulouse, France) by isotope dilution, gas chromatography, inductively coupled plasma mass spectrometry (ID-GC-ICPMS). Details about the methodology are available in Heimbürger et al. (2015). A total of fourteen stations (0-500 m depth) located in the ARCHm province and distributed along a transect at 15°S and between 160°E and 170°W were considered for analysis. Data obtained from the different water profiles were pooled at each depth to get a unique spatially integrated MeHg water depth profile representative of the ARCHm province. This profile aims at being compared to Hg concentrations in blood and muscle tissues of different tuna species occupying different vertical habitats in the same region.

Statistical analyses

All analyses were performed with the statistical open source R software (R Core Team, 2018). To visually investigate the spatial patterns of THg concentrations and $\delta^{15}N$ values in bigeye and yellowfin, we used generalized additive models (GAM), fitted with the *mgcv* package (Wood and Wood, 2015). Separated models were built per tuna species and tissue. Smoothed spatial contour maps were generated by fitting two dimensional thin plate regression splines on catch sample location (i.e., s(longitude, latitude)). We used a Gaussian family with an identity link function for both total Hg concentrations and $\delta^{15}N$ values. Linear correlations of THg concentrations and $\delta^{15}N$ values between blood and muscle tissues were assessed for bigeye and yellowfin tunas with Pearson correlation's coefficients.

To test for tissue-specific differences of THg concentrations in bigeye, yellowfin, albacore, and skipjack tunas from ARCHm (the only province with samples for the four different species), we used paired Wilcoxon tests with a Bonferroni correction of p-values. Then we used the ratio of THg concentrations between blood and muscle (blood to muscle ratio) to investigate differences in Hg distribution among tissues. Species-specific differences of blood to muscle THg ratios within ARCHm were tested considering the four tuna species with a Kruskal Wallis test, followed by a post-hoc Dunn test with a Bonferroni correction of p-values. For each species from ARCHm, we also investigated the relationship between blood to muscle THg ratios and muscle THg concentrations by fitting segmented regression models with *segmented* R package.

A set of generalized linear mixed models (GLMMs) were performed to evaluate the effect of four fixed factors on tuna THg concentrations: fish length, province (ARCHm and WARMm), tissue type (blood and muscle) and species (bigeye and yellowfin). GLMMs allow modelling non-normal data to evaluate the effect of a treatment whereas accounting for random effects (Bolker, 2009). The individual identifier was included as a random factor in our random intercept models to account for the non-independence of the data, since THg concentrations in blood and muscle tissues were measured in the same individual. We used the *glmer* function from *lme4* package (Bolker et al., 2021) to perform the model with a Gamma distribution and

246 "log" link function. Model selection was performed by reducing full models stepwise
247 and using the Akaike Information Criterion corrected by size (AICc, Burnham and
248 Anderson, 2004) and the Bayesian Information Criterion (BIC, Neath and Cavanaugh,
249 2012). To select the best-fit models, we evaluated the change in AICc relative to the
250 best AICc model (ΔAICc). Only models with ΔAICc <2 and with biological/ecological
251 coherence were selected (Burnham and Anderson, 2004, 2002). The coefficient of
252 determination (R^2) was obtained for the best model with highest support using the
253 function *rsquaredGLMM* from the *MuMin* package (Barton, 2020; Nakagawa et al.,
254 2017). Then, the best-fit model was visually verified for over-dispersion from residuals
255 diagnostic plots. Finally, the marginal effects of each factor and/or interactions on the
256 response variable were represented using the *plot_model* function from the *sjPlot*
257 package (Lüdecke, 2018).

258 We used linear regression to evaluate the link between THg levels in the four
259 tuna species from ARCHm and water dissolved MeHg concentrations at the
260 corresponding tuna foraging depth. The mean foraging depth during the day of each
261 tuna species was estimated following Evans et al. (2011), Houssard et al. (2017), and
262 Williams et al. (2015), and we considered the mean dissolved MeHg water
263 concentrations at the closest estimated tuna foraging depth.

Results and discussion

Capturing representative geographical trends in tuna blood and muscle tissues

Our results show a latitudinal gradient in the Western and Central Pacific Ocean for THg concentrations and $\delta^{15}N$ values in blood and muscle tissues of both bigeye and yellowfin tunas (Fig. 1). These trends confirm the results of Houssard et al. (2017, 2019) who also found a similar latitudinal gradient using larger datasets of tuna muscle tissues. Our results show that the same trend exists in blood from these same species. This latitudinal trend was attributed to tuna displaying a deeper vertical habitat in the ARCHm province where they are expected to forage more on mesopelagic preys enriched in Hg compared to WARMm (Houssard et al., 2019). On the other hand, the latitudinal gradient of $\delta^{15}N$ values in tuna muscle tissues was shown to reflect the spatial variability of particulate organic matter $\delta^{15}N$ values (Houssard et al., 2017), with lower values in ARCHm likely due to the presence of dinitrogen fixers that display low $\delta^{15}N$ values close to 0 ‰ (Bonnet et al., 2017; Garcia et al., 2007). Our results (i.e., higher THg concentrations in the south related to lower tuna $\delta^{15}N$ values) are also consistent with the findings of Médieu et al. (2021) who showed that the interannual occurrence of diazotrophic blooms in this region, characterized by low particulate organic matter $\delta^{15}N$ values, was associated with enhanced tuna Hg concentrations for the same years. These regional conditions could favor in situ MeHg production and bioavailability for the local food webs.

Regarding differences between blood and muscle tissues, for both THg concentrations and $\delta^{15}N$ values, we found the same spatial patterns (Figs. 1) and a high correlation between blood and muscle tissues in bigeye (Pearson coefficient correlation of 0.947 and 0.961 for THg concentrations and $\delta^{15}N$ values, respectively) (Figs. 1A-B, S1A and S1B) and yellowfin tunas (Pearson coefficient correlation of 0.699 and 0.953 for THg concentrations and $\delta^{15}N$ values, respectively) (Figs. 1C-D, and Figs. S1C and S1D). This indicates that despite having different turnover rates, the two tissues capture similar spatial trends. This reinforces the idea that these two species display relatively restricted movements and high site fidelity behavior in the western Pacific Ocean, compared to more mobile tuna species like bluefin tunas (Fonteneau and Hallier, 2015; Rooker et al., 2016). These results indicate that blood, which can be collected with non-lethal techniques, is also a good candidate to decipher spatial variations of THg

concentrations (and $\delta^{15}N$ values) in tunas. As such, both tissues are highly relevant matrices to study Hg geographical trends in bigeye and yellowfin.

Tuna species-specific mercury distribution in blood and muscle tissues

The best-fit GLMM ($R^2 = 0.95$) evaluating the effects of species, tissue type, fish length and province, as well as their combined interactions, on tuna THg concentrations, revealed that all four stand-alone factors were significant. As found visually with the spatial contour maps (Fig. 1) and discussed above, THg concentrations in ARCHm were significantly higher than in WARMm for both bigeye and yellowfin. Bigeye exhibited significantly higher THg concentrations than yellowfin, in both tissues. In blood, THg concentrations were 11 times higher in bigeye than in yellowfin (1.77 ± 2.30 µg.g^{-1} dw and 0.16 ± 0.14 µg.g^{-1} dw, respectively), while in muscle, bigeye THg concentrations were twice higher than those in yellowfin (1.20 ± 1.32 µg.g^{-1} dw, and 0.54 ± 0.45 µg.g^{-1} dw, respectively). Significant differences were also found between tissues, with higher THg concentrations measured in blood than in muscle for bigeye, while the opposite pattern was found in yellowfin. The best-fit GLMM shows that differences of THg concentrations between muscle and blood tissues depend on the province (significant interaction between species, tissue, and province). Specifically, significant differences of THg concentrations between tissues were generally observed in both species and provinces, with the exception for tissues of bigeye in WARMm (Fig. 2A). These differences were larger in ARCHm than in WARMm for both species. The model also suggests that differences of Hg accumulation between tissues and species also depend on fish individual length (significant interaction between species, tissue, and length). Total Hg concentrations in blood and muscle tissues of bigeye were found to increase similarly with fish length, while for yellowfin, THg concentrations were positively related to fish length in muscle only (Fig. 2B). Our results in bigeye contradict the absence of a relationship between fish length and blood THg concentrations observed by Kai et al. (1988) for the two same species. This contrasted result for bigeye tuna may be explained by a smaller sample size ($n = 12$), and/or a more restricted fish length range (94 – 126 cm) of individuals in Kai et al. (1988) (Fig. S2), compared to our dataset (n= 53; 60-160 cm, considering data from ARCHm and WARMm used in the GLMM analysis).

The tuna species-specific differences in Hg accumulation between blood and muscle tissues could result from a different kinetic exchange between these two compartments, suggesting that each tuna species might display tissue-specific Hg accumulation pathways. Harley et al. (2015) observed different correlations between fish length and THg concentrations depending on tissues (i.e., muscle, liver, heart, and kidney), suggesting heterogeneous dynamics of transport, and storage of Hg compounds in each tissue in sculpin fish from the Bering Sea.

When focusing on the ARCHm province only, and including skipjack and albacore tunas for a broader comparison, we also found significant differences of THg concentrations between tissues (Fig. 3A). Total Hg concentrations were higher in the muscle relative to blood tissue for skipjack, yellowfin, and albacore, while bigeye showed the opposite trend with higher values in blood (paired Wilcoxon test, p-value < 0.05) (Fig. 3A). The blood to muscle THg ratio was found to increase in the following order: skipjack < yellowfin < albacore < bigeye (Fig. 3B), and was significantly higher in bigeye compared to the three other species that were not different from each other (Dunn test, p-value < 0.05). Skipjack, the most epipelagic tuna species, showed the lowest mean blood to muscle THg ratio (~0.23) indicating an important and preferential enrichment of Hg in the muscle compartment relative to blood. Conversely, bigeye, the most mesopelagic species, exhibited the highest mean ratio (~1.71) showing Hg concentrations enriched in blood compared to muscle (Fig. 3B). Considering the differences of vertical habitat (Choy et al., 2009; Olson et al., 2016) and activity cost (Trudel and Rasmussen, 1997) of the four studied species, these results suggest that blood is increasingly enriched in Hg relative to muscle with expanding access into the deeper mesopelagic zone. The differences of blood to muscle THg ratios could also result from the variability in the tissue composition, such as lipid content in muscle (e.g., Hg dilution effect associated to lipid accumulation) (Balshaw et al., 2008). The four tuna species studied here exhibit relatively similar white muscle fat content (6.9 ± 4.9 %, 6.1 ± 4.7 %, 4.0 ± 3.8 %, and 9.2 ± 6.0 %, for bigeye, yellowfin, skipjack and albacore tunas respectively, L. Couturier unpub. data) suggesting that this factor has limited influence. Variation in hemoglobin levels in blood and/or binding properties could also explain our observations, since MeHg is known to display a strong affinity to hemoglobin thiol groups (Giblin and Massaro, 1975; Vahter et al., 1994; Pedrero Zayas et al., 2014). While no data are available for skipjack and albacore, yellowfin and

bigeye tunas also show similar hemoglobin concentrations (Brown, 1962; Lowe et al., 2000). However, Lowe and coworkers (2000) also revealed that bigeye display unique hemoglobin-oxygen binding properties, being able to capture twice more oxygen compared to the hemoglobin of the three other species. The context of enhanced oxygen binding hemoglobin properties for this mesopelagic tuna species with the known strong affinity of MeHg for the same proteins could explain the higher MeHg accumulation in blood compared to muscle in bigeye.

Species-specific differences in MeHg intake due to contrasted foraging behavior and depth could also trigger a change in the physiologic kinetics of Hg detoxification/accumulation when a threshold level is reached. Such idea has been developed for sea bass in Abreu et al. (2000), who observed higher Hg concentrations in muscle than in liver when Hg levels in fish muscle was low (below approximately 0.5 $\mu g.g^{-1}$), and the inverse relationship between the two tissues when muscle Hg concentrations were higher than ~1 $\mu g.g^{-1}$. Here, using segmented regression models, we found a significant breakpoint for bigeye only (p-value < 0.1, not significant for the three other species), at a muscle THg concentration of 0.72 ± 0.27 $\mu g.g^{-1}$ dw (Fig. S3). This suggests that above this threshold and for bigeye only, Hg tends to accumulate more in blood than in muscle. Bigeye individuals forage preferentially on deep myctophids and squids (Young et al., 2010) enriched in MeHg (Choy et al., 2009; Houssard et al., 2017; Madigan et al., 2018), whereas yellowfin, skipjack and to a lesser extent albacore almost exclusively feed on lower MeHg epipelagic preys (Olson et al., 2016). Then, if we hypothesize the existence of a threshold of Hg accumulation tolerance in muscle of bigeye, under conditions of high MeHg availability in the deeper habitat from ARCHm, THg concentrations would increase over this threshold causing an apparent limitation of accumulation in muscle while it would continue increasing in blood. This could also explain the higher difference in THg concentrations between blood and muscle in ARCHm where the foraging habitat of bigeye tuna is deeper than in WARMm (Fig. 2A, Houssard et al., 2017).

Muscle tissue is generally considered as a storage compartment for MeHg accumulating over tuna lifetime. The new finding from this study indicates a progressive enrichment and contribution of blood MeHg towards muscle MeHg in relation to tuna foraging depth. This result suggests that blood compartment is important towards understanding the origin of tuna Hg concentrations and

bioaccumulation in the light of oceanic MeHg production and concentrations with depth.

Tuna mercury concentrations mirror seawater methylmercury concentrations

We observed an increase in tuna muscle Hg concentrations with their depth of occurrence (Fig. 4A), which corroborates previous findings (Blum et al., 2013; Choy et al., 2009). This confirms that MeHg concentrations and accumulation in tunas are related to their foraging behavior, which is consistent with the increase of oceanic MeHg concentrations with depth. Additionally, the depth of occurrence of the four-tuna species and their corresponding blood and muscle THg concentrations mirror the MeHg depth profile in the water column (Fig. 4, R^2 of the regression was 0.57 and 0.46 for muscle and blood, respectively; p-values: 0.001 and <0.001, respectively). The spatially integrated high-resolution water MeHg depth profile in ARCHm is consistent with other profiles in the southern Pacific Ocean, although not exactly located in the same area (Munson et al., 2015). This profile shows that MeHg concentrations increase progressively with depth, ranging between 40 fM at the subsurface (20 m depth) up to 350 fM at 600 m depth approximately. Hence, most of the difference in the species-specific tuna THg concentrations is directly correlated to the corresponding MeHg concentrations at their depth of occurrence. This suggests that seawater baseline MeHg concentrations at the species depth of occurrence is a key relevant predictor of the distribution of Hg concentrations among tuna species.

The steep relationship between MeHg concentrations in water and tuna tissues, and in particular the higher enrichment of THg in blood relative to muscle in species inhabiting deeper waters, may support the possibility of a complementary contribution of waterborne MeHg uptake through the gills mediated by blood, in particular for bigeye. This route of exposure could complement the dietary intake of MeHg which is assumed to be predominant, and at a rate increasing with tuna foraging depth. This hypothesis is consistent with recent findings showing that tuna trophic position estimates are not a primary variable explaining the spatiotemporal trends of Hg concentrations in yellowfin, bigeye, and skipjack from the study region (Houssard et al., 2019; Médieu et al., 2022, 2021) and in bluefin tuna at larger oceanic scales (Tseng et al., 2021). For instance, experimental studies (mostly involving freshwater fishes) on

waterborne MeHg uptake show that MeHg concentrations in muscle also respond linearly to dissolved MeHg concentrations (Boddington et al., 1979; Hall et al., 1997). However, these studies found that waterborne MeHg uptake despite being significant, is limited (10-20%), relative to dietary MeHg representing the majority of MeHg intake (80-90%). Furthermore, tuna species present unique morphologic and physiologic features that may increase MeHg water uptake due to their unique gill morphometrics favoring oxygen transfer and the largest relative gill surface areas of any fish group, having up to 4-10 higher ventilation rates than freshwater fishes and other marine teleosts (Wegner et al., 2010). Wang et al. (2011) showed that fish MeHg direct uptake through the gills is controlled by swimming speed and respiration rates. Yellowfin and bigeye tunas display fast swimming speed and high mouth gape when foraging in hypoxic waters at the depth of oxygen minimum zone to increase ventilation volume (Bushnell and Brill, 1991; Gooding et al., 1981). These unique physiological adaptations that ensure oxygen uptake and metabolism may possibly enhange theuptake of water MeHg concentrations through the gills, especially at mesopelagic depth with the 5 fold increase in MeHg concentration at the mean foraging range of bigeye during the day (≈200 fM, 400 m depth, Fig. 4A) compared to the surface waters (≈40 fM, 20 m depth). Cossa et al. (1994) hypothesized that diffusion of dissolved gaseous dimethylmercury (which accounts for about half of total MeHg at depth) through the gills could be a significant pathway for MeHg accumulation, in addition to dietary intake. Further experimental and field studies, e.g., including measurement of Hg concentrations in other tissues (gills), and Hg stable isotopes in the water column could help elucidate the species-specific traits related to the uptake of dissolved water compounds in Hg accumulation in fish, and its contribution relative to dietary MeHg.

Conclusion

Total Hg concentrations in tunas is a promising marker to study MeHg distribution in the ocean, and the potential consequences to human health. Here, we present the first evidence of consistency in the spatial distribution patterns of THg concentrations in blood and muscle tissues in two tropical tuna species from the Western and Central Pacific Ocean. Our results highlight the pertinence of these two tissues for large-scale Hg monitoring studies. In particular, blood is a promising non-lethal marker of Hg distribution in tunas, such as its currently used in bird and mammal species from other oceanic regions. Furthermore, as THg concentrations in yellowfin

blood do not vary with fish length, contrary to muscle, the use of this tissue may overcome the biases associated to sampling fish length when using muscle tissues, allowing wider comparisons.

Our results reinforce the idea that habitat depth coupled with dissolved MeHg concentrations are key parameters to explain tuna species-specific differences of THg concentrations. Although dietary MeHg uptake is considered the predominant incorporation pathway of MeHg in tuna, further investigations would be valuable to help quantify the relative importance of waterborne MeHg. This is especially true for tunas foraging in mesopelagic environments exhibiting higher MeHg levels than in epipelagic waters and displaying unique blood binding properties.

We conclude that it is important not only to consider inter-specific differences, but also intra-specific tissue variations of the dynamic of Hg accumulation when evaluating Hg content among fish species. In addition, in predatory fishes such as tunas, habitat depth seems to play a fundamental role in Hg accumulation. The positive linear relationship found between tuna Hg concentrations and *in situ* seawater MeHg concentrations offers perspectives to predict the spatiotemporal evolutions of Hg in top predators by using models simulating both seawater and tuna Hg levels. Such model developments could help refine Hg predictions in top predators according to different climate change and Hg emissions scenarios, as recommended by the Minamata Convention.

Available dataset: Barbosa R., V., Point, D., Médieu, A., Allain, V., Gillikin, D.P., Munaron, J-M., Roupsard, F., Lorrain, A., 2022. Mercury concentration and nitrogen isotope values of muscle and blood tissues in tuna species from the Southwestern Pacific ocean. SEANOE. https://doi.org/10.17882/88179

Acknowledgments: We thank the French National Research Agency ANR-17-CE34-0010 project 'Unraveling the origin of methylMERcury TOXin in marine ecosystems' (MERTOX, PI DP) and VACOPA to AL for providing financial support for Hg analysis. We are grateful to the Western Central Pacific Fisheries Commission (WCPFC) and the Pacific Community (SPC) for providing access to tissue samples from the Pacific Marine Specimen Bank (https://www.spc.int/ofp/PacificSpecimenBank). We thank C. Sanchez and C. Cuewapuru for their help with tuna sampling and Laure Laffont from GET for Hg analyses and Anouk Verheyden and Madelyn Miller from Union College for isotope analyzes. LIEC was supported by the LabexMER (ANRH10HLABXH19) and co-funded by a grant from the French government ("Investissements d'Avenir" program), by a grant from the Regional Council of Brittany (SAD program), and by the EU FP7 Marie Curie actions (PCOFUND-GA-2013-609102), through the PRESTIGE program. DPG thanks the U.S. National Science Foundation for funding Union College's isotope ratio mass spectrometer and peripherals (NSF-MRI #1229258).

References

Abreu, S.N., Pereira, E., Vale, C., 2000. Accumulation of mercury in Sea bass from a contaminated lagoon (Ria de Aveiro, Portugal). Marine Pollution Bulletin 40, 5. https://doi.org/10.1016/S0025-326X(99)00187-3

Balshaw, S., Edwards, J.W., Ross, K.E., Daughtry, B.J., 2008. Mercury distribution in the muscular tissue of farmed southern bluefin tuna (Thunnus maccoyii) is inversely related to the lipid content of tissues. Food Chemistry 111, 616–621. https://doi.org/10.1016/j.foodchem.2008.04.041

Barton, K., 2020. Package "MuMIn". R package version 1.43.17.

Bearhop, S., Ruxton, G.D., Furness, R.W., 2000. Dynamics of mercury in blood and feathers of great skuas. Environmental Toxicology and Chemistry 19, 1638–1643. https://doi.org/10.1002/etc.5620190622

Bell, J.D., Allain, V., Allison, E.H., Andréfouët, S., Andrew, N.L., Batty, M.J., Blanc, M., Dambacher, J.M., Hampton, J., Hanich, Q., Harley, S., Lorrain, A., McCoy, M., McTurk, N., Nicol, S., Pilling, G., Point, D., Sharp, M.K., Vivili, P., Williams, P., 2015. Diversifying the use of tuna to improve food security and public health in Pacific Island countries and territories. Marine Policy 51, 584–591. https://doi.org/10.1016/j.marpol.2014.10.005

Block, B.A., Jonsen, I.D., Jorgensen, S.J., Winship, A.J., Shaffer, S.A., Bograd, S.J., Hazen, E.L., Foley, D.G., Breed, G.A., Harrison, A.-L., Ganong, J.E., Swithenbank, A., Castleton, M., Dewar, H., Mate, B.R., Shillinger, G.L., Schaefer, K.M., Benson, S.R., Weise, M.J., Henry, R.W., Costa, D.P., 2011. Tracking apex marine predator movements in a dynamic ocean. Nature 475, 86–90. https://doi.org/10.1038/nature10082

Bloom, N.S., 1992. On the Chemical Form of Mercury in Edible Fish and Marine Invertebrate Tissue. Canadian Journal of Fisheries and Aquatic Sciences 49, 1010–1017. https://doi.org/10.1139/f92-113

Blum, J.D., Popp, B.N., Drazen, J.C., Anela Choy, C., Johnson, M.W., 2013. Methylmercury production below the mixed layer in the North Pacific Ocean. Nature Geoscience 6, 879–884. https://doi.org/10.1038/ngeo1918

Boddington, M.J., Mackenzie, B.A., deFreitas, A.S.W., 1979. A respirometer to measure the uptake efficiency of waterborne contaminants in fish. Ecotoxicology and Environmental Safety 3, 383–393. https://doi.org/10.1016/0147-6513(79)90028-9

Bolker, B., 2009. GLMM on symbiont effects on coral predation.

Bolker, B., Maechler, M., Walker, S., Christensen, R.H.B., Skov, H., Dai, B., Scheipl, F., Grothendieck, G., Green, P., Fox, J., Bauer, A., Krivitsky, P.N., 2021. Package "lme4," CRAN.

Bonnet, S., Caffin, M., Berthelot, H., Moutin, T., 2017. Hot spot of N2 fixation in the western tropical South Pacific pleads for a spatial decoupling between N2 fixation and denitrification. Proc Natl Acad Sci USA 114, E2800–E2801. https://doi.org/10.1073/pnas.1619514114

Brown, W.D., 1962. The Concentration of Myoglobin and Hemoglobin in Tuna Flesh. Journal of Food Science 27, 26–28. https://doi.org/10.1111/j.1365-2621.1962.tb00052.x

Burnham, K.P., Anderson, D.R., 2004. Multimodel Inference: Understanding AIC and BIC in Model Selection. Sociological Methods & Research 33, 261–304. https://doi.org/10.1177/0049124104268644

Burnham, K.P., Anderson, D.R., 2002. Model Selection and Multimodel Inference: A Practical Information-Theoretic Approach, 2nd ed. Springer-Verlag, New York. https://doi.org/10.1007/b97636

Bushnell, P.G., Brill, R.W., 1991. Responses of Swimming Skipjack (Katsuwonus pelamis) and Yellowfin (Thunnus albacares) Tunas to Acute Hypoxia, and a Model of Their

552 Cardiorespiratory Function. Physiological Zoology 64, 787–811.
553 https://doi.org/10.1086/physzool.64.3.30158207
554 Campbell, L., Carpenter, E.J., Montoya, J.P., Kustka, A.B., Capone, D.G., 2005. Picoplankton
555 community structure within and outside a Trichodesmium bloom in the southwestern
556 Pacific Ocean. Vie et Mileu 55, 185–195.
557 Chavez, F.P., Buck, K.R., Barber, R.T., 1990. Phytoplankton taxa in relation to primary
558 production in the equatorial Pacific. Deep Sea Research Part A. Oceanographic
559 Research Papers 37, 1733–1752. https://doi.org/10.1016/0198-0149(90)90074-6
560 Chouvelon, T., Brach-Papa, C., Auger, D., Bodin, N., Bruzac, S., Crochet, S., Degroote, M.,
561 Hollanda, S.J., Hubert, C., Knoery, J., Munschy, C., Puech, A., Rozuel, E., Thomas, B.,
562 West, W., Bourjea, J., Nikolic, N., 2017. Chemical contaminants (trace metals,
563 persistent organic pollutants) in albacore tuna from western Indian and south-eastern
564 Atlantic Oceans: Trophic influence and potential as tracers of populations. Science of
565 The Total Environment 596–597, 481–495.
566 https://doi.org/10.1016/j.scitotenv.2017.04.048
567 Choy, C.A., Popp, B.N., Kaneko, J.J., Drazen, J.C., 2009. The influence of depth on mercury
568 levels in pelagic fishes and their prey. Proceedings of the National Academy of Sciences
569 106, 13865–13869. https://doi.org/10.1073/pnas.0900711106
570 Cossa, D., Martin, J.-M., Sanjuan, J., 1994. Dimethylmercury formation in the Alboran Sea.
571 Marine Pollution Bulletin 28, 381–384. https://doi.org/10.1016/0025-326X(94)90276-3
572 Evans, K., Patterson, T., Pedersen, M., 2011. Movement patterns of yellowfin tuna in the Coral
573 Sea region: defining connectivity with stocks in the western Pacific Ocean region.
574 CSIRO Marine and Atmospheric Research.
575 http://hdl.handle.net/102.100.100/104126?index=1
576 Fonteneau, A., Hallier, J.-P., 2015. Fifty years of dart tag recoveries for tropical tuna: A global
577 comparison of results for the western Pacific, eastern Pacific, Atlantic, and Indian
578 Oceans. Fisheries Research 163, 7–22. https://doi.org/10.1016/j.fishres.2014.03.022
579 Garcia, N., Raimbault, P., Sandroni, V., 2007. Seasonal nitrogen fixation and primary
580 production in the Southwest Pacific: nanoplankton diazotrophy and transfer of
581 nitrogen to picoplankton organisms. Mar. Ecol. Prog. Ser. 343, 25–33.
582 https://doi.org/10.3354/meps06882
583 Giblin, F.J., Massaro, E.J., 1975. The erythrocyte transport and transfer of methylmercury to
584 the tissues of the rainbow trout (Salmo gairdneri). Toxicology 5, 243–254.
585 https://doi.org/10.1016/0300-483X(75)90121-3
586 Gooding, R.M., Neill, W.H., Dizon, A.E., 1981. Respiration rates and low-oxygen tolerance limits
587 in Skipjack tuna, Katsuwonus pelamis. Fishery Bulletin 79, 31–48.
588 Graham, B.S., Koch, P.L., Newsome, S.D., McMahon, K.W., Aurioles, D., 2010. Using Isoscapes
589 to Trace the Movements and Foraging Behavior of Top Predators in Oceanic
590 Ecosystems, in: West, J.B., Bowen, G.J., Dawson, T.E., Tu, K.P. (Eds.), Isoscapes.
591 Springer Netherlands, Dordrecht, pp. 299–318. https://doi.org/10.1007/978-90-481-
592 3354-3_14
593 Hall, B.D., Bodaly, R.A., Fudge, R.J.P., Rudd, J.W.M., Rosenberg, D.M., 1997. Food as the
594 Dominant Pathway of Methylmercury Uptake by Fish. Water, Air, & Soil Pollution 100,
595 13–24. https://doi.org/10.1023/A:1018071406537
596 Harley, J., Lieske, C., Bhojwani, S., Castellini, J.M., López, J.A., O'Hara, T.M., 2015. Mercury and
597 methylmercury distribution in tissues of sculpins from the Bering Sea. Polar Biol 38,
598 1535–1543. https://doi.org/10.1007/s00300-015-1716-x
599 Heimbürger, L.-E., Sonke, J.E., Cossa, D., Point, D., Lagane, C., Laffont, L., Galfond, B.T.,
600 Nicolaus, M., Rabe, B., van der Loeff, M.R., 2015. Shallow methylmercury production in
601 the marginal sea ice zone of the central Arctic Ocean. Sci Rep 5, 10318.
602 https://doi.org/10.1038/srep10318

603 Houssard, P., Lorrain, A., Tremblay-Boyer, L., Allain, V., Graham, B.S., Menkes, C.E.,
604 Pethybridge, H., Couturier, L.I.E., Point, D., Leroy, B., Receveur, A., Hunt, B.P.V.,
605 Vourey, E., Bonnet, S., Rodier, M., Raimbault, P., Feunteun, E., Kuhnert, P.M.,
606 Munaron, J.-M., Lebreton, B., Otake, T., Letourneur, Y., 2017. Trophic position
607 increases with thermocline depth in yellowfin and bigeye tuna across the Western and
608 Central Pacific Ocean. Progress in Oceanography 154, 49–63.
609 https://doi.org/10.1016/j.pocean.2017.04.008
610 Houssard, P., Point, D., Tremblay-Boyer, L., Allain, V., Pethybridge, H., Masbou, J., Ferriss, B.E.,
611 Baya, P.A., Lagane, C., Menkes, C.E., Letourneur, Y., Lorrain, A., 2019. A Model of
612 Mercury Distribution in Tuna from the Western and Central Pacific Ocean: Influence of
613 Physiology, Ecology and Environmental Factors. Environmental Science & Technology
614 53, 1422–1431. https://doi.org/10.1021/acs.est.8b06058
615 Kai, N., Ueda, T., Takeda, Y., Kataoka, A., 1988. The levels of mercury and selenium in blood of
616 tunas. Bulletin of the Japanese Society of Scientific Fisheries 54, 1981–1985.
617 https://eurekamag.com/research/021/950/021950266.php
618 Keva, O., Hayden, B., Harrod, C., Kahilainen, K.K., 2017. Total mercury concentrations in liver
619 and muscle of European whitefish (Coregonus lavaretus (L.)) in a subarctic lake -
620 Assessing the factors driving year-round variation. Environmental Pollution 231, 1518–
621 1528. https://doi.org/10.1016/j.envpol.2017.09.012
622 Kojadinovic, J., Potier, M., Le Corre, M., Cosson, R.P., Bustamante, P., 2007. Bioaccumulation of
623 trace elements in pelagic fish from the Western Indian Ocean. Environmental
624 Pollution, Lichens in a Changing Pollution Environment 146, 548–566.
625 https://doi.org/10.1016/j.envpol.2006.07.015
626 Kwon, S.Y., Blum, J.D., Madigan, D.J., Block, B.A., Popp, B.N., 2016. Quantifying mercury
627 isotope dynamics in captive Pacific bluefin tuna (Thunnus orientalis). Elem Sci Anth 4,
628 000088. https://doi.org/10.12952/journal.elementa.000088
629 Le Borgne, R., Allain, V., Griffiths, S.P., Matear, R.J., McKinnon, A.D., Richardson, A.J., Young,
630 J.W., 2011. Vulnerability of open ocean food webs in the tropical Pacific to climate
631 change, in: Vulnerability of Tropical Pacific Fisheries and Aquaculture to Climate
632 Change. Secretariat of the Pacific Community, New Caledonia, pp. 189–249.
633 Lee, C.-S., Lutcavage, M.E., Chandler, E., Madigan, D.J., Cerrato, R.M., and Fisher, N.S., 2016.
634 Declining mercury concentrations in bluefin tuna reflect reduced emissions to the
635 North Atlantic Ocean. Environmental Science and Technology 50, 12825-12830.
636 Leblanc, K., Cornet, V., 2018. Biogenic and lithogenic particulate silica, diatom abundance and
637 C biomass data during the OUTPACE (2015) cruise. https://doi.org/10.17882/55743
638 Logan, J.M., Pethybridge, H., Lorrain, A., Somes, C.J., Allain, V., Bodin, N., Choy, C.A., Duffy, L.,
639 Goñi, N., Graham, B., Langlais, C., Ménard, F., Olson, R., Young, J., 2020. Global
640 patterns and inferences of tuna movements and trophodynamics from stable isotope
641 analysis. Deep Sea Research Part II: Topical Studies in Oceanography 175, 104775.
642 https://doi.org/10.1016/j.dsr2.2020.104775
643 Longhurst, A.R., 2007. Ecological Geography of the Sea. Academic Press, Amsterdam, Boston,
644 MA.
645 Lowe, T.E., Brill, R.W., Cousins, K.L., 2000. Blood oxygen-binding characteristics of bigeye tuna
646 (Thunnus obesus), a high-energy-demand teleost that is tolerant of low ambient
647 oxygen. Marine Biology 136, 1087–1098. https://doi.org/10.1007/s002270000255
648 Lüdecke, D., 2018. ggeffects: Tidy Data Frames of Marginal Effects from Regression Models.
649 Journal of Open Source Software 3, 772. https://doi.org/10.21105/joss.00772
650 Madigan, D.J., Li, M., Yin, R., Baumann, H., Snodgrass, O.E., Dewar, H., Krabbenhoft, D.P.,
651 Baumann, Z., Fisher, N.S., Balcom, P., Sunderland, E.M., 2018. Mercury Stable Isotopes
652 Reveal Influence of Foraging Depth on Mercury Concentrations and Growth in Pacific
653 Bluefin Tuna. Environ. Sci. Technol. 52, 6256–6264.
654 https://doi.org/10.1021/acs.est.7b06429

Mason, R.P., Fitzgerald, W.F., 1990. Alkylmercury species in the equatorial Pacific. Nature 347, 457–459. https://doi.org/10.1038/347457a0

Médieu, A., Point, D., Itai, T., Angot, H., Buchanan, P.J., Allain, V., Fuller, L., Griffiths, S., Gillikin, D.P., Sonke, J.E., Heimbürger-Boavida, L.-E., Desgranges, M.-M., Menkes, C.E., Madigan, D.J., Brosset, P., Gauthier, O., Tagliabue, A., Bopp, L., Verheyden, A., Lorrain, A., 2022. Evidence that Pacific tuna mercury levels are driven by marine methylmercury production and anthropogenic inputs. PNAS 119. https://doi.org/10.1073/pnas.2113032119

Médieu, A., Point, D., Receveur, A., Gauthier, O., Allain, V., Pethybridge, H., Menkes, C.E., Gillikin, D.P., Revill, A.T., Somes, C.J., Collin, J., Lorrain, A., 2021. Stable mercury concentrations of tropical tuna in the south western Pacific ocean: An 18-year monitoring study. Chemosphere 263, 128024. https://doi.org/10.1016/j.chemosphere.2020.128024

Moisander, P.H., Beinart, R.A., Hewson, I., White, A.E., Johnson, K.S., Carlson, C.A., Montoya, J.P., Zehr, J.P., 2010. Unicellular Cyanobacterial Distributions Broaden the Oceanic N2 Fixation Domain. Science 327, 1512–1514. https://doi.org/10.1126/science.1185468

Munson, K.M., Lamborg, C.H., Swarr, G.J., Saito, M.A., 2015. Mercury species concentrations and fluxes in the Central Tropical Pacific Ocean. Global Biogeochemical Cycles 29, 656–676. https://doi.org/10.1002/2015GB005120

Nakagawa, S., Johnson, P.C.D., Schielzeth, H., 2017. The coefficient of determination R2 and intra-class correlation coefficient from generalized linear mixed-effects models revisited and expanded. Journal of The Royal Society Interface 14, 20170213. https://doi.org/10.1098/rsif.2017.0213

Neath, A.A., Cavanaugh, J.E., 2012. The Bayesian information criterion: background, derivation, and applications. WIREs Computational Statistics 4, 199–203. https://doi.org/10.1002/wics.199

Nicklisch, S.C.T., Bonito, L.T., Sandin, S., Hamdoun, A., 2017. Mercury levels of yellowfin tuna (Thunnus albacares) are associated with capture location. Environmental Pollution 229, 87–93. https://doi.org/10.1016/j.envpol.2017.05.070

Olson, R.J., Young, J.W., Ménard, F., Potier, M., Allain, V., Goñi, N., Logan, J.M., Galván-Magaña, F., 2016. Chapter Four: Bioenergetics, Trophic Ecology, and Niche Separation of Tunas, in: Advances in Marine Biology. Elsevier, pp. 199–344. https://doi.org/10.1016/bs.amb.2016.06.002

Outridge, P.M., Mason, R.P., Wang, F., Guerrero, S., Heimbürger-Boavida, L.E., 2018. Updated Global and Oceanic Mercury Budgets for the United Nations Global Mercury Assessment 2018. Environ. Sci. Technol. 52, 11466–11477. https://doi.org/10.1021/acs.est.8b01246

Pedrero Zayas, Z., Ouerdane, L., Mounicou, S., Lobinski, R., Monperrus, M., Amouroux, D., 2014. Hemoglobin as a major binding protein for methylmercury in white-sided dolphin liver. Analytical and Bioanalytical Chemestry 406**,** 1121–1129. https://doi.org/10.1007/s00216-013-7274-6

R Core Team, 2018. R: A language and environment for statistical computing; 2015. Vienna, Austria. URL https://www.R-project.org/.

Rooker, J.R., Wells, R.J.D., Itano, D.G., Thorrold, S.R., Lee, J.M., 2016. Natal origin and population connectivity of bigeye and yellowfin tuna in the Pacific Ocean. Fisheries Oceanography 25, 277–291. https://doi.org/10.1111/fog.12154

Shiozaki, T., Kodama, T., Furuya, K., 2014. Large-scale impact of the island mass effect through nitrogen fixation in the western South Pacific Ocean. Geophysical Research Letters 41, 2907–2913. https://doi.org/10.1002/2014GL059835

Sirot, V., Leblanc, J.-C., Margaritis, I., 2012. A risk–benefit analysis approach to seafood intake to determine optimal consumption. Br J Nutr 107, 1812–1822. https://doi.org/10.1017/S0007114511005010

Storelli, M.M., Stuffler, R.G., Marcotrigiano, G.O., 2002. Total and methylmercury residues in tuna-fish from the Mediterranean sea. Food Additives & Contaminants 19, 7.
Sunderland, E.M., 2007. Mercury Exposure from Domestic and Imported Estuarine and Marine Fish in the U.S. Seafood Market. Environmental Health Perspectives 115, 235–242. https://doi.org/10.1289/ehp.9377
Sunderland, E.M., Li, M., Bullard, K., 2018. Decadal Changes in the Edible Supply of Seafood and Methylmercury Exposure in the United States. Environmental Health Perspectives 126, 017006. https://doi.org/10.1289/EHP2644
Trudel, M., Rasmussen, J.B., 1997. Modeling the Elimination of Mercury by Fish. Environ. Sci. Technol. 31, 1716–1722. https://doi.org/10.1021/es960609t
Tseng, C.-M., Ang, S.-J., Chen, Y.-S., Shiao, J.-C., Lamborg, C.H., He, X., Reinfelder, J.R., 2021. Bluefin tuna reveal global patterns of mercury pollution and bioavailability in the world's oceans. Proceedings of the National Academy of Sciences 6.
Vahter, M., Mottet, N.K., Friberg, L., Lind, B., Shen, D.D., Burbacher, T., 1994. Speciation of Mercury in the Primate Blood and Brain Following Long-Term Exposure to Methyl Mercury. Toxicology and Applied Pharmacology 124, 221–229. https://doi.org/10.1006/taap.1994.1026
Wang, F., Outridge, P.M., Feng, X., Meng, B., Heimbürger-Boavida, L.-E., Mason, R.P., 2019. How closely do mercury trends in fish and other aquatic wildlife track those in the atmosphere? - Implications for evaluating the effectiveness of the Minamata Convention. Science of the Total Environment 674, 58–70. https://doi.org/10.1016/j.scitotenv.2019.04.101
Wang, R., Wong, M.-H., Wang, W.-X., 2011. Coupling of methylmercury uptake with respiration and water pumping in freshwater tilapia Oreochromis niloticus. Environmental Toxicology and Chemistry 30, 2142–2147. https://doi.org/10.1002/etc.604
Wegner, N.C., Sepulveda, C.A., Bull, K.B., Graham, J.B., 2010. Gill morphometrics in relation to gas transfer and ram ventilation in high-energy demand teleosts: Scombrids and billfishes. Journal of Morphology 271, 36–49. https://doi.org/10.1002/jmor.10777
Williams, A.J., Allain, V., Nicol, S.J., Evans, K.J., Hoyle, S.D., Dupoux, C., Vourey, E., Dubosc, J., 2015. Vertical behavior and diet of albacore tuna (Thunnus alalunga) vary with latitude in the South Pacific Ocean. Deep Sea Research Part II: Topical Studies in Oceanography 113, 154–169. https://doi.org/10.1016/j.dsr2.2014.03.010
Wood, S., Wood, M.S., 2015. Package "mgcv". R package version 1.
World Health Organization, UNEP Chemicals, 2008. Guidance for identifying populations at risk from mercury exposure. UNEP DTIE Chemicals Branch and WHO Department of Food Safety, Zoonoses and Foodborne Diseases, Geneva, Switzerland.
Young, J.W., Lansdell, M.J., Campbell, R.A., Cooper, S.P., Juanes, F., Guest, M.A., 2010. Feeding ecology and niche segregation in oceanic top predators off eastern Australia. Mar Biol 157, 2347–2368. https://doi.org/10.1007/s00227-010-1500-y

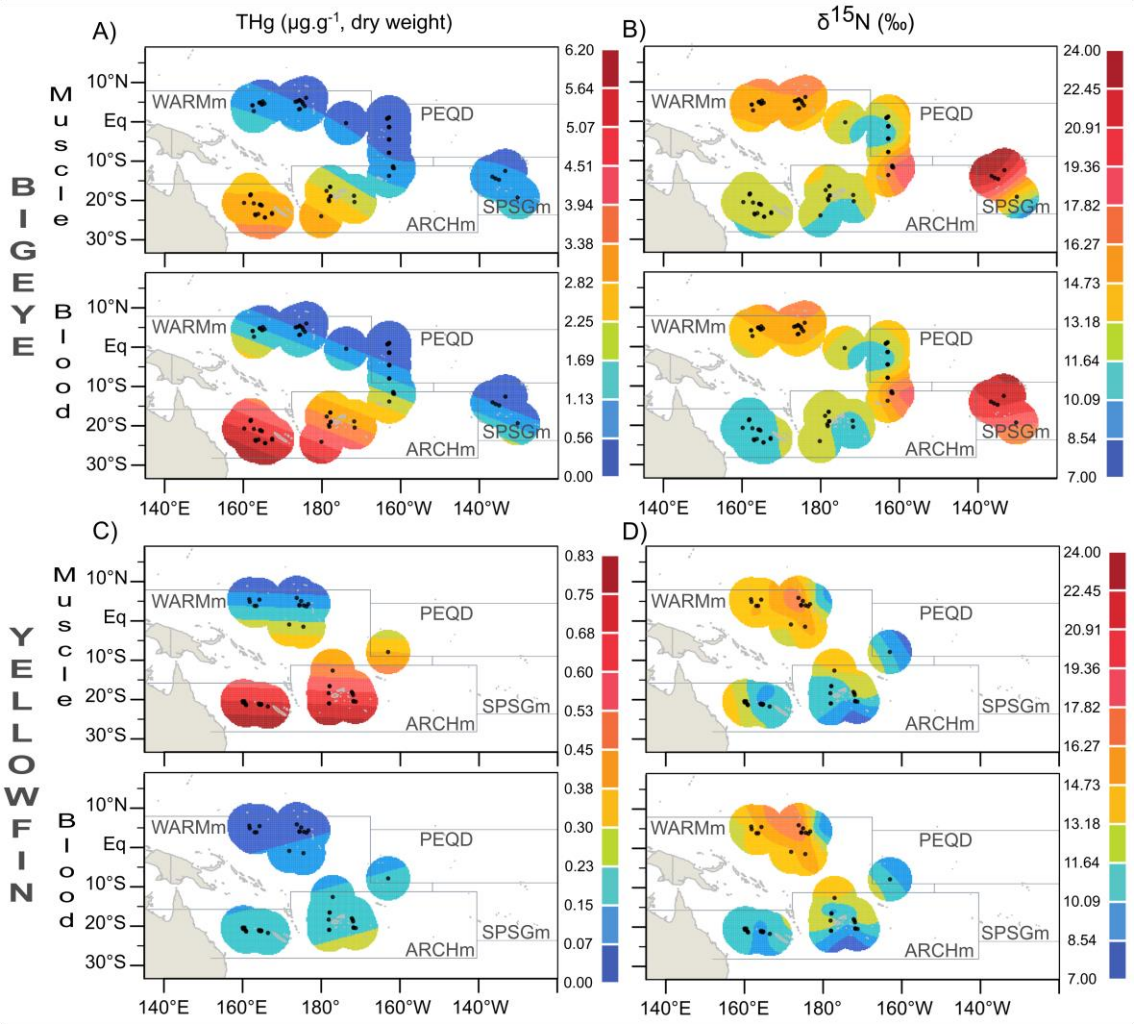

748

749 **Figure 1**. Smoothed spatial contour maps of muscle and blood total mercury (THg)
750 concentrations in A) bigeye, and C) yellowfin tunas (note that the scale for THg
751 concentrations is different between the two species); and their corresponding $\delta^{15}N$
752 values for B) bigeye, and D) yellowfin tunas through the Western and Central Pacific
753 Ocean. Black dots represent tuna sampling locations. Grey lines delineate
754 biogeochemical provinces as described in Houssard et al. (2017): ARCHm =
755 Archipelagic deep basins modified province, PEQD = Pacific Equatorial Divergence
756 province, SPSGm = South Pacific Subtropical Gyre modified province, and WARMm =
757 Warm Pool modified province.

758

759

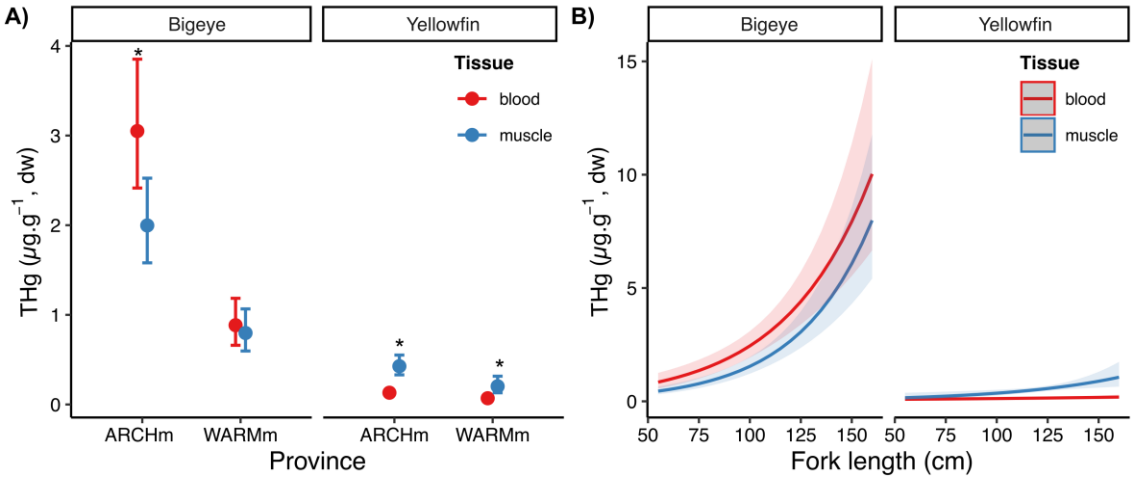

760 **Figure 2.** Total mercury (THg) predicted concentrations and relationships with
761 explanatory variables from our best-fit GLMM. A) THg concentrations in muscle (blue)
762 and blood (red) tissues by province and species while taking into account the size effect.
763 Dots and whiskers indicate means and 95% confidence intervals respectively. B)
764 Relationship between blood and muscle THg concentrations and fish length in both
765 bigeye and yellowfin tunas when removing the province effect. (*) indicates significant
766 differences between tissues. The coloured shadows show the 95% confidence intervals.
767 Relationship between THg concentrations and fork length was significant, except in
768 yellowfin blood.

769

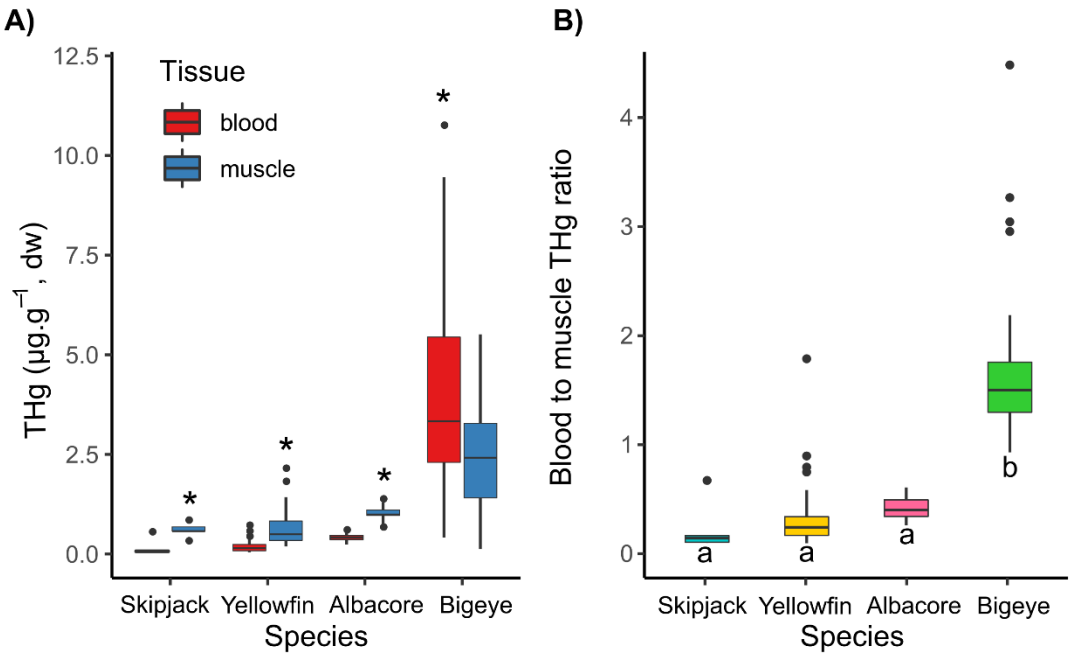

770 **Figure 3.** Boxplots of A) Total mercury content (THg, µg.g^{-1}, dw) in muscle and blood
771 tissue, and B) blood to muscle THg ratio in bigeye, yellowfin, albacore and skipjack
772 from the ARCHm province. * indicates significant differences between tissues and 'a'
773 and 'b' letters indicate significant different groups. The central horizontal line is the
774 median value, the box contains 50% of the values, and the whiskers above and below
775 the box indicate the variability outside the upper and lower quantiles respectively.
776 Points are outliers.
777

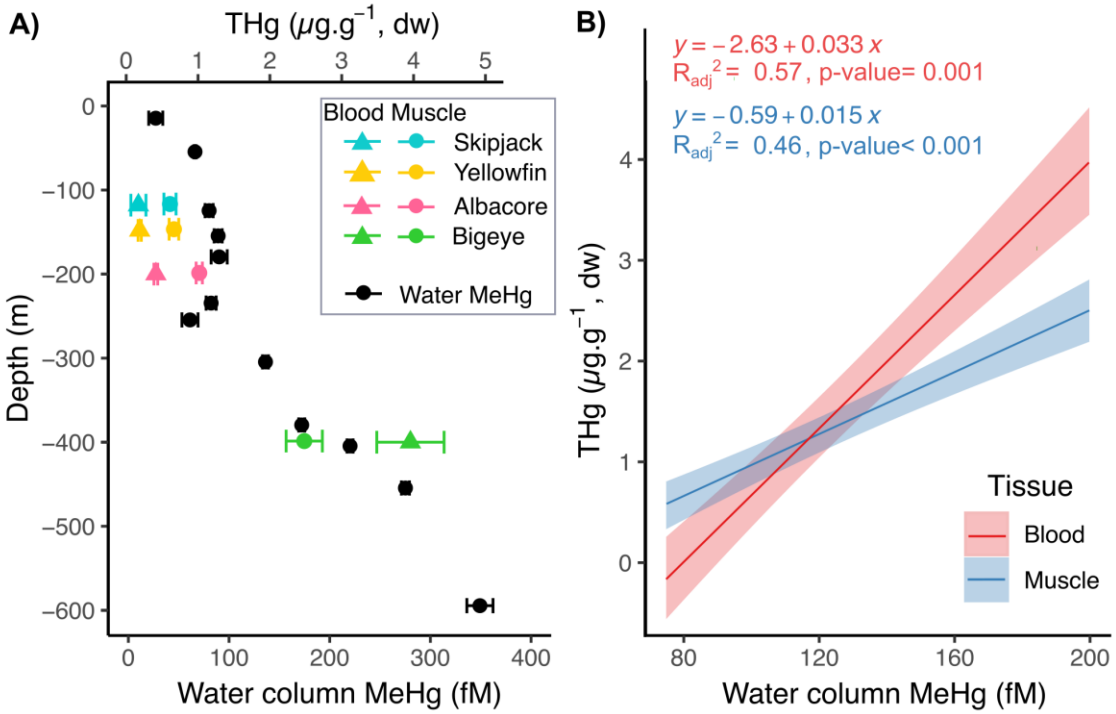

778

779 **Figure 4.** A) Mean values (± standard error) of water column MeHg concentrations in
780 relation to depth in the ARCHm province; and mean values (± se) of THg
781 concentrations in muscle (colored circles) and blood (colored triangles) of tuna species
782 in relation to their mean depth distribution in the Western and Central Pacific Ocean. B)
783 Regression between THg concentrations in blood and muscle tissues of the four studied
784 tuna species in ARCHm and the corresponding mean water dissolved MeHg content at
785 the species mean depth of occurrence. The colored shadows show the 95% confidence
786 intervals.